Published in final edited form as:
Dent Mater. 2013 February ; 29(2): 199–210. doi:10.1016/j.dental.2012.10.005.

Novel dental adhesives containing nanoparticles of silver and amorphous calcium phosphate

Mary Anne S. Melo[1,2], **Lei Cheng**[1,3], **Ke Zhang**[1,4], **Michael D. Weir**[1], **Lidiany K. A. Rodrigues**[2], and **Hockin H. K. Xu**[1,5,6,7]

[1]Biomaterials & Tissue Engineering Division, Dept. of Endodontics, Prosthodontics and Operative Dentistry, University of Maryland Dental School, Baltimore, MD 21201, USA

[2]Faculty of Pharmacy, Dentistry and Nursing, Federal University of Ceara, Fortaleza, CE, Brazil

[3]State Key Laboratory of Oral Diseases, West China College of Stomatology, Sichuan University, Chengdu, China

[4]Dept. of Orthodontics, School of Stomatology, Capital Medical University, Beijing, China

[5]Center for Stem Cell Biology & Regenerative Medicine, University of Maryland School of Medicine, Baltimore, MD 21201, USA

[6]Marlene and Stewart Greenebaum Cancer Center, University of Maryland School of Medicine, Baltimore, MD 21201, USA

[7]Dept. of Mechanical Engineering, Univ. of Maryland, Baltimore County, MD 21250, USA

Abstract

Objectives—Secondary caries is the main reason for restoration failure, and replacement of the failed restorations accounts for 50–70% of all restorations. Antibacterial adhesives could inhibit residual bacteria in tooth cavity and invading bacteria along the margins. Calcium (Ca) and phosphate (P) ion release could remineralize the lesions. The objectives of this study were to incorporate nanoparticles of silver (NAg) and nanoparticles of amorphous calcium phosphate (NACP) into adhesive for the first time, and to investigate the effects on dentin bond strength and plaque microcosm biofilms.

Methods—Scotchbond Multi-Purpose adhesive was used as control. NAg were added into primer and adhesive at 0.1% by mass. NACP were mixed into adhesive at 10%, 20%, 30% and 40%. Microcosm biofilms were grown on disks with primer covering the adhesive on a composite. Biofilm metabolic activity, colony-forming units (CFU) and lactic acid were measured.

Results—Human dentin shear bond strengths (n=10) ranged from 26 to 34 MPa; adding NAg and NACP into adhesive did not decrease the bond strength ($p > 0.1$). SEM examination revealed resin tags from well-filled dentinal tubules. Numerous NACP infiltrated into the dentinal tubules. While NACP had little antibacterial effect, NAg in bonding agents greatly reduced the biofilm viability and metabolic activity, compared to the control ($p < 0.05$). CFU for total microorganisms,

Correspondence: Prof. Hockin H. K. Xu (hxu@umaryland.edu), Director of Biomaterials & Tissue Engineering Division, Department of Endodontics, Prosthodontics and Operative Dentistry, University of Maryland Dental School, Baltimore, MD 21201. Prof. Lidiany K. A. Rodrigues (lidianykarla@yahoo.com), Faculty of Pharmacy, Dentistry and Nursing, Federal University of Ceara, Fortaleza, CE, Brazil.

total streptococci, and mutans streptococci on bonding agents with NAg were an order of magnitude less than those of the control. Lactic acid production by biofilms for groups containing NAg was 1/4 of that of the control.

Significance—Dental plaque microcosm biofilm viability and acid production were greatly reduced on bonding agents containing NAg and NACP, without compromising dentin bond strength. The novel method of incorporating dual agents (remineralizing agent NACP and antibacterial agent NAg) may have wide applicability to other dental bonding systems.

Keywords

Antibacterial adhesive; dentin bond strength; silver nanoparticles; calcium phosphate nanoparticles; human saliva microcosm biofilm; caries inhibition

1. Introduction

Extensive studies have been undertaken to improve dental composites with advances in filler compositions and resin chemistry [1–5]. The property enhancements have enabled composites to be increasingly used as esthetic filling materials [6–8]. Indeed, recent data showed that composite restorations represented the highest percentage among three categories: 77.3 million restorations (46.6%) were composites, 52.5 million (31.6%) were amalgams, and 36.2 million (21.8%) were crowns, totaling 166 million restorations placed in the USA in 2005 [9]. However, a major shortcoming of composites is that they accumulate more biofilms and plaques *in vivo,* compared to other restorative materials [10]. The acid production by biofilms can lead to secondary caries especially at the tooth-restoration margins [11–15]. Recurrent caries is the main reason for restoration failure, and replacement of the failed restorations accounts for 50–70% of all restorations performed [11].

To address this problem, novel antibacterial dental composites were developed [16–20]. Quaternary ammonium monomers, such as 12-methacryloyloxydodecylpyridinium bromide (MDPB), were copolymerized in resins to yield antibacterial activities [16,21,22]. Another class of antibacterial composites incorporated silver (Ag) particles [23,24]. For example, a composite containing Ag inhibited *S. mutans* growth and had a long-lasting antibacterial activity [24]. Ag nanoparticles were highly effective for antibacterial applications [25,26]. Resins containing Ag nanoparticles were recently reported that inhibited biofilm viability and growth [20,27,28].

The development of composites containing calcium phosphate (CaP) particles with remineralization capabilities represents an important approach to inhibiting secondary caries [29–32]. These composites could release supersaturating levels of calcium (Ca) and phosphate (P) ions and remineralize enamel and dentin lesions [30,32]. Traditional CaP composites contained CaP particles of several microns in sizes [29,30,32]. Recently, CaP nanoparticles of sizes of about 100 nm were synthesized via a spray-drying technique and filled into dental composites [31,33]. These nanocomposites achieved Ca and P ion release similar to those of traditional CaP composites, while possessing much better mechanical properties [31,33].

Besides composites, it is also important to develop adhesives capable of inhibiting secondary caries. Adhesives bond the composite to dentin and infiltrate into dentinal tubules and a demineralized layer to form an interlocked interface [34,35]. Vast efforts have been made to enhance adhesive bonding to the tooth structure [36–38]. Clinically, residual bacteria could exist in the prepared tooth cavity. In addition, microleakage could allow bacteria to invade the tooth-restoration interfaces. Therefore, it is desirable for the adhesive

to be antibacterial to inhibit recurrent caries [16,18,39,40]. Antibacterial agents such as MDPB [16,39], methacryloxylethyl cetyl dimethyl ammonium chloride [40], and cetylpyridinium chloride [18] were used to develop antibacterial adhesives. In addition, dental primer directly contacts the tooth structure and could kill residual bacterial if rendered antibacterial [21,22,41]. However, a literature search revealed only a small number of publications on antibacterial adhesives and primers [16,18,21,22,39,40]. While nanoparticles of amorphous calcium phosphate (NACP) were incorporated into composite with Ca and P ion release [43,44], and the release of Ca and P ions were shown to remineralize tooth lesions [30,32], NACP have not been incorporated into bonding agents.

The objective of this study was to incorporate NAg and NACP into a bonding system for the first time, and to investigate the antibacterial properties using a dental plaque microcosm biofilm model. While previous studies established the Ca and P ion release with enamel and dentin remineralization [30,32], the present study focused on the effect of NAg and NACP on dentin bond strength and antibacterial activity. The hypotheses were: (1) Incorporating NACP at mass fractions of 10–40% into the adhesive would not decrease the shear bond strength to human dentin, compared to control with 0% NACP; (2) Incorporating NAg into primer and adhesive would not decrease the dentin shear bond strength; (3) NACP (being a remineralizing agent) would have little antibacterial effect, while NAg would have a strong antibacterial effect.

2. Materials and methods

2.1. NAg incorporation into primer and adhesive

Scotchbond Multi-Purpose (3M, St. Paul, MN), referred to as “SBMP”, was used as the parent bonding system to test the effect of incorporation of NACP and NAg. The purpose was to investigate a model system, and then the method of incorporating NACP and NAg could be applied to other bonding agents. According to the manufacturer, SBMP etchant contained 37% phosphoric acid. SBMP primer single bottle contained 35–45% 2-Hydroxyethylmethacrylate (HEMA), 10–20% copolymer of acrylic and itaconic acids, and 40–50% water. SBMP adhesive contained 60–70% BisGMA and 30–40% HEMA.

Silver 2-ethylhexanoate powder (Strem, New Buryport, MA) was dissolved in 2-(tert-butylamino)ethyl methacrylate (TBAEMA, Sigma) at 0.08 g of silver salt per 1 g of TBAEMA, following previous studies [27,28]. TBAEMA was used because it improves the solubility by forming Ag-N coordination bonds with Ag ions, thereby facilitating the Ag salt to dissolve in the resin solution. TBAEMA was selected since it contains reactive methacrylate groups and can be chemically incorporated into a resin upon photopolymerization. This method produced NAg with a mean particle size of 2.7 nm that were well dispersed in the resin [27,28]. To incorporate NAg into the primer, the aforementioned Ag-TBAEMA solution was mixed with the SBMP primer at a silver 2-ethylhexanoate/(primer + silver 2-ethylhexanoate) of 0.1% by mass; this mass fraction was selected based on previous studies [27,28]. To incorporate NAg into the adhesive, the Ag-TBAEMA was mixed with the SBMP adhesive at 0.1% mass fraction.

2.2. Addition of NACP into adhesive

Nanoparticles of ACP ($Ca_3[PO_4]_2$) were synthesized using a spray-drying technique as described previously [31,42]. Briefly, calcium carbonate ($CaCO_3$, Fisher, Fair Lawn, NJ) and dicalcium phosphate anhydrous ($CaHPO_4$, Baker Chemical, Phillipsburg, NJ) were dissolved into an acetic acid solution to obtain final Ca and P ionic concentrations of 8 mmol/L and 5.333 mmol/L, respectively. The Ca/P molar ratio for the solution was 1.5, the same as that for ACP. The solution was sprayed into the heated chamber of the spray-drying

apparatus. The dried particles were collected via an electrostatic precipitator (AirQuality, Minneapolis, MN), yielding NACP with a mean particle size of 116 nm [43].

The NACP were mixed with the adhesive containing 0.1% silver 2-ethylhexanoate. The NACP mass fractions in the adhesive were: 0%, 10%, 20%, 30%, and 40%, following previous studies on NACP nanocomposites [43,44]. To compare the differences in the viscosity of the various adhesive resin-NACP pastes, a previous flow method was adapted, because the flow of the paste is inversely related to the viscosity [6,45]. Briefly, 0.1 g of each adhesive paste was placed on a glass slide and the diameter of the adhesive drop was measured, yielding the area A_{before}. A second glass slide was placed on the top, a 100 g weight was applied for 5 min for the paste to flow, and the diameter of the adhesive paste was measured again, yielding the area A_{after}. The change in area was calculated: $\Delta A = (A_{after} - A_{before})/A_{before}$. A smaller ΔA corresponded to a higher viscosity. Six measurements were made for each adhesive (n = 6).

2.3. Dentin shear bond strength testing and SEM examination

Six bonding agents were tested:

1. SBMP primer, SBMP adhesive (termed “SBMP control”).
2. Primer+0.1% NAg, adhesive+0.1% NAg (termed “P&A+NAg”. P = primer, A = adhesive).
3. Primer+0.1% NAg, adhesive+0.1% NAg+10% NACP (“P+NAg, A+NAg +10NACP”).
4. Primer+0.1% NAg, adhesive+0.1% NAg+20% NACP (“P+NAg, A+NAg +20NACP”).
5. Primer+0.1% NAg, adhesive+0.1% NAg+30% NACP (“P+NAg, A+NAg +30NACP”).
6. Primer+0.1% NAg, adhesive+0.1% NAg+40% NACP (“P+NAg, A+NAg +40NACP”).

Extracted caries-free human third molars were cleaned and stored in 0.01% thymol solution. The tips of the molar crowns were cut off via a diamond saw (Isomet, Buehler, Lake Bluff, IL) to yield flat mid-coronal dentin surfaces. Following a previous study [46], the tooth was embedded in a poly-carbonate holder (Bosworth, Skokie, IL) and ground perpendicular to the longitudinal axis using 320-grit SiC paper until there was no occlusal enamel left. The bonding procedures are shown in Fig. 1A. Briefly, the dentin surface was etched with 37% phosphoric acid gel for 15 s and rinsed with water for 15 s [46]. The primer was applied with a brush-tipped applicator and rubbed in for 15 s, and the solvent was removed with a stream of air. The adhesive was then applied and photo-cured for 10 s (Optilux VCL 401, Demetron Kerr**,** Danbury**,** CT). Then, a stainless-steel iris with a central opening (diameter = 4 mm, thickness = 1.5 mm) was held against the adhesive-treated dentin surface. The central opening was filled with a composite (TPH, Caulk/Dentsply, Milford, DE) and photo-cured for 60 s.

The bonded specimens were stored in distilled water at 37 °C for 24 h [46]. Then, the dentin shear bond strength, S_D, was measured as schematically shown in Fig. 1B. The chisel was connected with a computer-controlled Universal Testing Machine (MTS, Eden Prairie, MN), held parallel to the composite-dentin interface, and loaded at 0.5 mm/min until the bond failed. S_D was calculated as: $S_D = 4P/(\pi d^2)$, where P is the load at failure, and d is the diameter of the composite. Ten teeth were tested for each group (n = 10).

For scanning electron microscopy (SEM) examination, the bonded tooth was cut through the center parallel to the longitudinal axis via a diamond saw (Isomet) with copious water. The sectioned surface was polished with increasingly finer SiC paper up to 4000 grit. Following a previous study [22], the polished surface was treated with 50% phosphoric acid for 30 s, then with 5% NaOCl for 10 min. After being thoroughly rinsed with water for 10 min, the specimens were air dried and then sputter-coated with gold. Three specimens were prepared for each group. The specimens were then examined in an SEM (Quanta 200, FEI, Hillsboro, OR).

2.4. Specimen fabrication for biofilm experiments

Following previous studies [21,40], layered disk specimens were made as shown in Fig. 3A. A polyethylene mold (inner diameter = 9 mm, thickness = 2 mm) was situated on a glass slide. A primer was applied into the mold to cover the glass. After drying with a stream of air, an adhesive was applied and cured for 20 s with Optilux. A composite (TPH) was placed on the adhesive to completely fill the mold, and light-cured for 1 min. The bonded specimens were immersed in water and agitated for 1 h to remove any uncured monomer [21]. The disks were then dried and sterilized with ethylene oxide (Anprolene AN 74i, Andersen, Haw River, NC).

2.5. Dental plaque microcosm model and live/dead assay

Saliva is ideal for growing dental plaque microcosm biofilms *in vitro* which maintain much of the complexity and heterogeneity of dental plaque *in vivo* [47]. The dental plaque microcosm model was approved by the University of Maryland. Saliva was collected from a healthy adult donor having natural dentition without active caries or periopathology, and without the use of antibiotics within the last 3 months [48]. The donor did not brush teeth for 24 h and abstained from food/drink intake for at least 2 h prior to donating saliva. Stimulated saliva was collected during parafilm chewing and kept on ice. The saliva was diluted in sterile glycerol to a concentration of 70%, and stored at −80 ºC [48].

The saliva-glycerol stock was added, with 1:50 final dilution, to a growth medium as inoculum. The growth medium contained mucin (type II, porcine, gastric) at a concentration of 2.5 g/L; bacteriological peptone, 2.0 g/L; tryptone, 2.0 g/L; yeast extract, 1.0 g/L; NaCl, 0.35 g/L, KCl, 0.2 g/L; $CaCl_2$, 0.2 g/L; cysteine hydrochloride, 0.1 g/L; haemin, 0.001 g/L; vitamin K1, 0.0002 g/L, at pH 7 [49]. The inoculum was cultured in an incubator (5% CO_2, 37 °C) for 24 h. Each disk was placed into a well of 24-well plates, with the primer on the top. Then, 1.5 mL of inoculum was added to each well, and incubated for 8 h. The disks were transferred to new 24-well plates with fresh medium and incubated. After 16 h, the disks were transferred to new 24-well plates with fresh medium and incubated for 24 h. This totaled 2 d of incubation, which was shown in a previous study to be sufficient to form microcosm biofilms [48].

Disks with 2-d biofilms were washed three times with phosphate buffered saline (PBS), and then stained using a live/dead bacterial kit (Molecular Probes, Eugene, OR). Live bacteria were stained with Syto 9 to produce a green fluorescence, and bacteria with compromised membranes were stained with propidium iodide to produce a red fluorescence. Specimens were examined with an epifluorescence microscope (TE2000-S, Nikon, Melville, NY). The area of green staining (live bacteria) was computed using NIS Elements imaging software (Nikon). The area fraction of live bacteria = green staining area/total area of the image. Six specimens were used for each group (n = 6). Three randomly-chosen fields of view were photographed from each specimen yielding a total of 18 images for each group.

2.6. MTT assay of metabolic activity

MTT (3-[4,5-Dimethylthiazol-2-yl]-2,5-diphenyltetrazolium bromide) assay was used to measure the metabolic activity of biofilms [28,50]. MTT is a colorimetric assay that measures the enzymatic reduction of MTT, a yellow tetrazole, to formazan. Each disk with the 2-d biofilm was transferred to a new 24-well plate. One mL of MTT dye (0.5 mg/mL MTT in PBS) was added to each well and incubated for 1 h. During this process, metabolically active bacteria reduced the MTT to purple formazan. After 1 h, the disks were transferred to a new 24-well plate, 1 mL of dimethyl sulfoxide (DMSO) was added to solubilize the formazan crystals, and the plate was incubated for 20 min in the dark. After mixing via pipetting, 200 μL of the DMSO solution from each well was transferred to a 96-well plate, and the absorbance at 540 nm (optical density OD540) was measured via a microplate reader (SpectraMax M5, Molecular Devices, Sunnvale, CA). A higher absorbance is related to a higher formazan concentration, which indicates a higher metabolic activity in the biofilm adherent on the disk.

2.7. Lactic acid production and colony-forming unit (CFU) counts

Disks with 2-d biofilms were rinsed with cysteine peptone water (CPW) to remove loose bacteria, and transferred to 24-well plates containing buffered peptone water (BPW) plus 0.2% sucrose. The samples were incubated for 3 h to allow the biofilms to produce acid. The BPW solutions were then stored for lactate analysis. Lactate concentrations were determined using an enzymatic (lactate dehydrogenase) method [48]. The microplate reader was used to measure the absorbance at 340 nm (optical density OD_{340}) for the collected BPW solutions. Standard curves were prepared using a lactic acid standard (Supelco, Bellefonte, PA).

Disks with biofilms were transferred into tubes with 2 mL CPW, and the biofilms were harvested by sonication and vortexing via a vortex mixer (Fisher, Pittsburgh, PA). Three types of agar plates were used. First, tryptic soy blood agar culture plates were used to determine total microorganisms [48]. Second, mitis salivarius agar (MSA) culture plates, containing 15% sucrose, were used to determine total streptococci [51]. This is because MSA contains selective agents crystal violet, potassium tellurite and trypan blue, which inhibit most gram-negative bacilli and gram-positive bacteria except streptococci, thus enabling streptococci to grow [51]. Third, cariogenic mutans streptococci are known to be resistant to bacitracin, and this property was used to isolate mutans streptococci from the oral microflora. The MSA agar plates with 0.2 units of bacitracin per mL were used to determine mutans streptococci.

One-way analysis of variance (ANOVA) was performed to detect the significant effects of the variables. Tukey's multiple comparison was used to compare the data at a p value of 0.05.

3. Results

Fig. 1 shows (A) schematic of the bonding procedures, (B) schematic of the bond test, and (C) human dentin shear bond strength data (mean ± sd; n = 10). Adding 0.1% NAg into primer and adhesive yielded a bond strength of (30.7 ± 8.3) MPa, similar to (30.2 ± 5.0) MPa for the control ($p > 0.1$). Further adding 10% NACP into the adhesive slightly increased the bond strength to (34.3 ± 7.7) MPa ($p > 0.1$). While 40% NACP slightly decreased the bond strength, all the six groups had bond strengths that were not significantly different ($p > 0.1$).

Typical SEM images of the dentin-adhesive interfaces are shown in Fig. 2 for (A) SBMP control, (B) P+NAg, A+NAg+20NACP, and (C) P+NAg, A+NAg+40NACP. Numerous resin tags "T" from well-filled dentinal tubules were visible in all the samples. The resin

tags were slightly shorter at 40% NACP than the other groups. “HL” refers to the hybrid layer between the adhesive and the underlying mineralized dentin. At a higher magnification, the NACP nanoparticles were visible in (D) with 20% NACP. Arrows in (D) indicate examples of NACP nanoparticles infiltrated into the dentinal tubules. This feature became more visible at higher magnifications in (E) and (F), where arrows indicate NACP, which infiltrated into not only the straight and smooth tubules (E), but also the bent and irregularly-shaped tubules (F).

The adhesive and hybrid layers of the bonded interface were examined at a higher magnification in Fig. 3 at (A) 20%, (B) 30% and (C) 40% of NACP. The NACP were readily visible in SEM in the adhesive and hybrid layers at 10% and 20% NACP. At 30% and 40% NACP, there was less contrast between the NACP and the resin matrix in the SEM; however, the NACP were still present, as indicated by the arrows in (B) and (C). The flow of the adhesives was measured, as the adhesive paste viscosity is inversely related to the flowability. Fig. 3D plots the measured area change for the adhesive paste (mean ± sd; n = 6). The area increase after the flow of the paste under 100 g of load was not significantly different from 0% to 30% NACP ($p > 0.1$). However, incorporation of 40% NACP significantly reduced the flow of the adhesive, yielding a smaller Δ A ($p < 0.05$).

Fig. 4 shows (A) a schematic of biofilm culture on the layered specimen, (B–G) live/dead staining images for the six groups. Biofilms adherent on the control disks were primarily alive with continuous green staining. In sharp contrast, biofilms adherent on A&P+NAg had substantial areas with red, yellow and orange staining, indicating that the biofilm viability was substantially compromised. Adding NACP from 10% to 40% mass fraction did not appear to significantly alter the biofilm appearance. All the disks modified with NAg and NACP were covered mainly with red and orange staining, with small areas of green staining.

Fig. 5A plots the live bacteria (green staining) area fraction. Incorporation of NAg into bonding agents decreased the live bacteria coverage by more than half, compared to the control ($p < 0.05$). The addition of NACP did not further reduce the live bacteria area fraction ($p > 0.1$). Fig. 5B plots the MTT metabolic results for the biofilms. Control disks had biofilms with a high metabolic activity. Incorporation of 0.1% of NAg decreased the metabolic activity by more than half ($p < 0.05$). Adding NACP to the adhesive did not further significantly decrease the metabolic activity, although there was a decreasing trend at 30% and 40% NACP ($p > 0.1$).

Fig. 6 plots biofilm CFU counts per disk for: (A) Total microorganisms, (B) total streptococci, and (C) mutans streptococci. NAg greatly reduced the CFU compared to that of the control ($p < 0.05$). Specimens with NAg and NACP reduced the CFU by an order of magnitude, compared to the control. Specimens with 40% NACP slightly reduced the CFU, compared to P&A+NAg without NACP; however, this decrease was not statistically significant ($p > 0.1$).

Fig. 7 plots the lactic acid production by biofilms. Biofilms on control disks produced the most acid, indicating that the un-modified commercial bonding agent was not antibacterial. Incorporation of NAg dramatically decreased the acid production, to less than half of that of the control ($p < 0.05$). Adding 30% or 40% NACP slightly and significantly ($p < 0.05$) decreased the acid production, compared to P&A+NAg without NACP. Lactic acid production by biofilms on the disks with 30% and 40% NACP were about 1/4 of the acid production for the control.

4. Discussion

This is the first report on incorporating NACP and NAg into bonding agents. NACP are a promising type of nano-fillers for composites to release high levels of Ca and PO_4 ions with remineralization potential, while the composite maintained good mechanical properties [43,44]. NAg are another type of promising fillers for dental resins, shown in recent studies with NAg of 2–3 nm in sizes [27,28]. Due to the small size and high surface area of the NAg, a strong antibacterial activity could be achieved at a low filler level, without adversely affecting the composite color and mechanical properties [27,28]. In the present study, NACP and NAg were incorporated into a bonding system for the first time. The rationale was to achieve the double benefits of remineralization and antibacterial properties. The present study demonstrated that it was feasible to incorporate NACP and NAg into bonding agent, yielding much lower biofilm viability and acid production, without significantly compromising dentin bond strength. The incorporation of 0.1% NAg into both primer and adhesive had no adverse effect on the bond strength, compared to the commercial control without NAg. The incorporation of 10%–30% NACP also had no adverse effect on bond strength. A previous study showed that a composite with 20% NACP released Ca and P ions to levels comparable to traditional CaP composites shown to effectively remineralize tooth lesions [43]. Another study showed that a composite with 30% NACP neutralized an acid attack, and raised the solution pH from a cariogenic pH of 4 to a safe pH of 6.5 [44]. Therefore, the incorporation of 0.1% NAg plus 20% or 30% NACP into the bonding agent is expected to provide antibacterial, acid neutralization and remineralization benefits. The method of incorporating dual agents (NACP as a remineralizing agent, and NAg as an antibacterial agent) may be applicable to a wide range of dental bonding systems.

Traditional CaP composites were filled with CaP particles of about 1–55 μm in sizes [29,30,32]. These composites released Ca and P ions and remineralized tooth lesions [30,32]. The spray-drying technique produced a new generation of CaP nanoparticles having sizes of around 100 nm with a high specific surface area. The resulting nanocomposites could have substantial releases of Ca and P ions, while possessing mechanical properties nearly two-fold those of traditional CaP composites [31,33]. The NACP nanocomposite greatly increased the ion release at a low pH, which in essence is a “smart” behavior as it provides ions when needed to combat caries [43]. The NACP nanocomposite was moderately antibacterial against planktonic *S. mutans*, likely because NACP was alkaline [44]. This is consistent with the present study which showed that the specimens containing 30% and 40% NACP caused a moderate decrease in MTT activity, CFU and lactic acid, although in most cases such a decrease was not statistically significant. Therefore, the main purpose of incorporating NACP was Ca and P ion release and remineralization, not antibacterial activity. One reason of using NACP, and not traditional CaP fillers, was that NACP could release more Ca and P ions at lower filler levels [43]. This is important because a low filler level could be used for adhesives so that the adhesive could maintain a low viscosity and the ability to flow into dentinal tubules. Another reason of using NACP was that particles of about 100 nm in sizes could infiltrate into dentinal tubules more easily than traditional CaP particles of several microns to tens of microns in sizes.

Besides Ca and P ions, there is a need for a potent antibacterial activity. Caries is a dietary carbohydrate-modified bacterial infectious disease caused by acid production by biofilms [13,14]. More than half of tooth cavity restorations placed by the dentists are replacements, with secondary caries as the main reason for failure [11,12,15]. An antibacterial bonding agent at the tooth-restoration interface is beneficial because there are often residual bacteria in the prepared tooth cavity [22,39,40]. There has been an increased interest in less removal of tooth structure and the minimal intervention dentistry [52], which could leave behind more carious tissues with active bacteria in the tooth cavity. Furthermore, the atraumatic

restorative treatment (ART) method has received increasing attention, which usually does not remove the carious tissues completely [53]. While the NACP could help remineralize the demineralized tooth structure, the NAg primer and adhesive could kill the residual bacteria. In addition, while a complete sealing of the tooth-restoration interface is highly desirable, it is difficult to achieve, as many studies showed microgaps at the interfaces which could allow for bacteria invasion [54,55]. Residual bacteria and new invading bacteria along the tooth-restoration margins could harm the pulp and cause recurrent caries. The primer directly contacts the dentin, and therefore could be an important vehicle to deliver antimicrobial agents such as NAg to kill bacteria in the tooth cavity including those in the dentinal tubules. Furthermore, microgaps were observed between the adhesive resin and the primed dentin, or between the adhesive resin and the hybrid layer [54,55]. This would suggest that a large portion of the marginal gap is surrounded by the cured adhesive resin, hence the invading bacteria would mostly come into contact with the adhesive surface [39]. Therefore, it is desirable to not only have an antibacterial primer, but also an antibacterial adhesive. Therefore, the present study incorporated NAg into both the adhesive and the primer. This study showed that the commercial adhesive without modification was not antibacterial, consistent with previous results showing that the cured commercial adhesives had normal bacteria growth with no antibacterial activity [39,40,56]. In contrast, the NAg primer-adhesive system greatly decreased the biofilm viability, reducing the CFU to nearly 1/10, and acid production to 1/4, of those of the commercial control.

Ag has a strong antibacterial activity [26], low toxicity and good biocompatibility with human cells [57], and a long-term antibacterial effect due to sustained silver ion release [25]. Composites containing Ag inhibited oral bacteria such as *S. mutans* [20,23,24,27]. Recently, Ag nanoparticles with a high surface area were incorporated into resins to reduce the Ag particle concentration necessary for efficacy, without compromising the composite color and mechanical properties [27,28]. Regarding the antibacterial mechanism, Ag ions could inactivate the vital enzymes of bacteria, thus causing DNA in the bacteria to lose its replication ability, which leads to cell death [26]. Regarding the durability, Ag-containing composites showed long-term antibacterial effects and inhibited *S. mutans* growth for more than 6 months [23]. The Ag salt was dissolved in the TBAEMA monomer in the present study, which was mixed with the resin and photo-cured, thus forming the NAg *in situ*. This yielded well-dispersed NAg in the resin without agglomeration [27,28], avoiding the need to mix pre-fabricated nanoparticles with the adhesive which could cause agglomeration.

The dentin shear bond strengths in this study ranged from 26 MPa with 40% NACP, to 34 MPa with 10% NACP. A previous study used the same bonding and testing procedures, and measured a dentin shear bond strength of about 20 MPa for a resin containing 40% of traditional ACP particles with 3 to 58 μm in sizes [46]. While polymer differences may have affected the bond strength, their ACP particles being much larger than the NACP likely also contributed to a lower bond strength than that of the present study. Regarding the test method, a recent article reviewed 100 studies published between 2007 and 2009 [58]. They found that most studies used bonding areas between 3 and 4 mm in diameter, consistent with the 4 mm in the present study. The most frequently used crosshead speeds were 0.5 and 1 mm/min [58]; the present study used 0.5 mm/min. Regarding sample size, previous studies used n as low as 5 and as high as 25, with the majority using n = 10 [58], which is the same as that of the present study. Previous studies tested commercial bonding agents and reported dentin shear bond strengths of 23 to 34 MPa for SBMP [59,60]. Hence the bond strengths of the present study are consistent with the previous reports. Regarding the scatter in the shear bond strength, the biological, chemical, microstructural variations and anisotropy in the extracted human teeth likely contributed to the standard deviation in the data. The standard deviation/mean in the present study ranged from 16% to 27%, which is consistent with previous studies [46,58–60]. The bonding agents appeared to have infiltrated and wetted the

dentin surface well, manifested by the formation of long resin tags from well-filled dentinal tubules. The successful infiltration of numerous nanoparticles into dentinal tubules is expected to exert therapeutic and remineralizing effects. The present study focused on the synthesis of novel NACP-NAg bonding agents and biofilm experiments, while measuring the dentin bond strength after 1 d of water-aging. Further study should determine the bond strength after long-term water-aging to investigate the effects of Ca and P ion release, remineralization, and antibacterial activity on the durability of the dentin-resin bond.

5. Conclusions

The present study incorporated NACP and NAg into bonding agent for the first time, yielding a potent antibacterial activity while maintaining a strong dentin bond strength. The rationale for adding NACP and NAg was to combine Ca and P ions from NACP with antibacterial activity from NAg to inhibit biofilms and caries. Adding 0.1% NAg and 10% to 40% NACP did not compromise the dentin bond strength. NACP was previously shown to have high levels of Ca and P ion release which could remineralize tooth lesions; the present study showed that NACP had little antibacterial activity. The antibacterial effect was provided by NAg, which reduced the CFU counts for total microorganisms, total streptococci, and mutans streptococci by an order of magnitude. Metabolic activity and lactic acid production were also greatly reduced. The antibacterial and NACP-containing bonding agents may help inhibit residual bacteria in the tooth cavity, hinder the invading bacteria along the margins, and remineralize lesions. The novel method of incorporating a remineralizing agent (NACP) and an antibacterial agent (NAg) together in the same adhesive may have wide applicability to other bonding systems and cements.

Acknowledgments

We thank Drs. Joseph M. Antonucci, Nancy J. Lin and Sheng Lin-Gibson of the National Institute of Standards and Technology, and Dr. Gary E. Schumacher and Anthony A. Giuseppetti of the Paffenbarger Research Center for discussions. We thank Esstech (Essington, PA) for donating the materials, and the technical support of the Core Imaging Facility of the University of Maryland Baltimore. This study was supported by NIH R01DE17974 and R01DE14190 (HX), seed fund (HX) from the University of Maryland School of Dentistry, scholarship from the Coordination for Improvement of Higher Education/Fulbright Doctoral Program BEX 0523/11-9 (MASM), National Natural Science Foundation of China grant 81100745 (LC), and financial support from the School of Stomatology at the Capital Medical University in China (KZ).

References

1. Lim BS, Ferracane JL, Sakaguchi RL, Condon JR. Reduction of polymerization contraction stress for dental composites by two-step light-activation. Dent Mater. 2002; 18:436–444. [PubMed: 12098572]
2. Watts DC, Marouf AS, Al-Hindi AM. Photo-polymerization shrinkage-stress kinetics in resin-composites: methods development. Dent Mater. 2003; 19:1–11. [PubMed: 12498890]
3. Lu H, Stansbury JW, Bowman CN. Impact of curing protocol on conversion and shrinkage stress. J Dent Res. 2005; 84:822–826. [PubMed: 16109991]
4. Xu X, Ling L, Wang R, Burgess JO. Formation and characterization of a novel fluoride-releasing dental composite. Dent Mater. 2006; 22:1014–1023. [PubMed: 16378636]
5. Drummond JL. Degradation, fatigue, and failure of resin dental composite materials. J Dent Res. 2008; 87:710–719. [PubMed: 18650540]
6. Bayne SC, Thompson JY, Swift EJ, Stamatiades P, Wilkerson M. A characterization of first-generation flowable composites. J Am Dent Assoc. 1998; 129:567–577. [PubMed: 9601169]
7. Ruddell DE, Maloney MM, Thompson JY. Effect of novel filler particles on the mechanical and wear properties of dental composites. Dent Mater. 2002; 18:72–80. [PubMed: 11740967]
8. Ferracane JL. Resin composite - State of the art. Dent Mater. 2011; 27:29–38. [PubMed: 21093034]

9. Beazoglou T, Eklund S, Hef ey D, Meiers J, Brown LJ, Bailit H. Economic impact of regulating the use of amalgam restorations. Public Health Reports. 2007; 122:657–663. [PubMed: 17877313]
10. Beyth N, Domb AJ, Weiss EI. An in vitro quantitative antibacterial analysis of amalgam and composite resins. J Dent. 2007; 35:201–206. [PubMed: 16996674]
11. Deligeorgi V, Mjor IA, Wilson NH. An overview of reasons for the placement and replacement of restorations. Prim Dent Care. 2001; 8:5–11. [PubMed: 11405031]
12. Jokstad A, Bayne S, Blunck U, Tyas M, Wilson N. Quality of dental restorations. FDI Commission Projects 2–95. International Dent J. 2001; 51:117–158.
13. Featherstone JD. The continuum of dental caries - Evidence for a dynamic disease process. J Dent Res. 2004; 83:C39–C42. [PubMed: 15286120]
14. ten Cate JM. Biofilms, a new approach to the microbiology of dental plaque. Odontology. 2006; 94:1–9. [PubMed: 16998612]
15. Sakaguchi RL. Review of the current status and challenges for dental posterior restorative composites: clinical, chemistry, and physical behavior considerations. Dent Mater. 2005; 21:3–6. [PubMed: 15680996]
16. Imazato S. Review: Antibacterial properties of resin composites and dentin bonding systems. Dent Mater. 2003; 19:449–457. [PubMed: 12837391]
17. Beyth N, Yudovin-Farber I, Bahir R, Domb AJ, Weiss EI. Antibacterial activity of dental composites containing quaternary ammonium polyethylenimine nanoparticles against Streptococcus mutans. Biomaterials. 2006; 27:3995–4002. [PubMed: 16564083]
18. Namba N, Yoshida Y, Nagaoka N, Takashima S, Matsuura-Yoshimoto K, Maeda H, et al. Antibacterial effect of bactericide immobilized in resin matrix. Dent Mater. 2009; 25:424–430. [PubMed: 19019421]
19. Thome T, Mayer MP, Imazato S, Geraldo-Martins VR, Marques MM. In vitro analysis of inhibitory effects of the antibacterial monomer MDPB-containing restorations on the progression of secondary rooth caries. J Dent. 2009; 37:705–711. [PubMed: 19540033]
20. Fan C, Chu L, Rawls HR, Norling BK, Cardenas HL, Whang K. Development of an antimicrobial resin - A pilot study. Dent Mater. 2011; 27:322–328. [PubMed: 21112619]
21. Imazato S, Ehara A, Torii M, Ebisu S. Antibacterial activity of dentine primer containing MDPB after curing. J Dent. 1998; 26:267–271. [PubMed: 9594480]
22. Imazato S, Tay FR, Kaneshiro AV, Takahashi Y, Ebisu S. An in vivo evaluation of bonding ability of comprehensive antibacterial adhesive system incorporating MDPB. Dent Mater. 2007; 23:170–176. [PubMed: 16469372]
23. Yoshida K, Tanagawa M, Atsuta M. Characterization and inhibitory effect of antibacterial dental resin composites incorporating silver-supported materials. J Biomed Mater Res. 1999; 4:516–522. [PubMed: 10497286]
24. Tanagawa M, Yoshida K, Matsumoto S, Yamada T, Atsuta M. Inhibitory effect of antibacterial resin composite against *Streptococcus mutans*. Caries Res. 1999; 33:366–371. [PubMed: 10460960]
25. Damm C, Munsted H, Rosch A. Long-term antimicrobial polyamide 6/silver nanocomposites. J Mater Sci. 2007; 42:6067–6073.
26. Rai M, Yada A, Gade A. Silver nanoparticles as a new generation of antimicrobials. Biotechnol Adv. 2009; 27:76–83. [PubMed: 18854209]
27. Cheng YJ, Zeiger DN, Howarter JA, Zhang X, Lin NJ, Antonucci JM, et al. In situ formation of silver nanoparticles in photocrosslinking polymers. J Biomed Mater Res B. 2011; 97:124–131.
28. Cheng L, Weir MD, Xu HHK, Antonucci JM, Kraigsley AM, Lin NJ, et al. Antibacterial amorphous calcium phosphate nanocomposite with quaternary ammonium salt and silver nanoparticles. Dent Mater. 2011 in review.
29. Skrtic D, Antonucci JM, Eanes ED, Eichmiller FC, Schumacher GE. Physiological evaluation of bioactive polymeric composites based on hybrid amorphous calcium phosphates. J Biomed Mater Res B. 2000; 53:381–391.
30. Dickens SH, Flaim GM, Takagi S. Mechanical properties and biochemical activity of remineralizing resin-based Ca-PO_4 cements. Dent Mater. 2003; 19:558–566. [PubMed: 12837405]

31. Xu HHK, Sun L, Weir MD, Antonucci JM, Takagi S, Chow LC. Nano dicalcium phosphate anhydrous-whisker composites with high strength and Ca and PO_4 release. J Dent Res. 2006; 85:722–727. [PubMed: 16861289]
32. Langhorst SE, O'Donnell JNR, Skrtic D. In vitro remineralization of enamel by polymeric amorphous calcium phosphate composite: Quantitative microradiographic study. Dent Mater. 2009; 25:884–891. [PubMed: 19215975]
33. Xu HHK, Weir MD, Sun L, Moreau JL, Takagi S, Chow LC, et al. Strong nanocomposites with Ca, PO_4 and F release for caries inhibition. J Dent Res. 2010; 89:19–28. [PubMed: 19948941]
34. Spencer P, Wang Y. Adhesive phase separation at the dentin interface under wet bonding conditions. J Biomed Mater Res. 2002; 62:447–456. [PubMed: 12209931]
35. Ikemura K, Tay FR, Endo T, Pashley DH. A review of chemical-approach and ultramorphological studies on the development of fluoride-releasing dental adhesives comprising new pre-reacted glass ionomer (PRG) fillers. Dent Mater J. 2008; 27:315–329. [PubMed: 18717159]
36. Park J, Eslick J, Ye Q, Misra A, Spencer P. The influence of chemical structure on the properties in methacrylate-based dentin adhesives. Dent Mater. 2011; 27:1086–1093. [PubMed: 21816460]
37. Pashley DH, Tay FR, Breschi L, Tjaderhane L, Carvalho RM, Carrilho M, et al. State of the art etch-and-rinse adhesives. Dent Mater. 2011; 27:1–16. [PubMed: 21112620]
38. Van Meerbeek B, Yoshihara K, Yoshida Y, Mine A, De Munck J. State of the art of self-etch adhesives. Dent Mater. 2011; 27:17–28. [PubMed: 21109301]
39. Imazato S, Kinomoto Y, Tarumi H, Ebisu S, Tay FR. Antibacterial activity and bonding characteristics of an adhesive resin containing antibacterial monomer MDPB. Dent Mater. 2003; 19:313–319. [PubMed: 12686296]
40. Li F, Chen J, Chai Z, Zhang L, Xiao Y, Fang M, et al. Effects of a dental adhesive incorporating antibacterial monomer on the growth, adherence and membrane integrity of Streptococcus mutans. J Dent. 2009; 37:289–296. [PubMed: 19185408]
41. Hiraishi N, Yiu CK, King NM, Tay FR. Effect of chlorhexidine incorporation into a self-etching primer on dentine bond strength of a luting cement. J Dent. 2010; 38:496–502. [PubMed: 20298738]
42. Chow LC, Sun L, Hockey B. Properties of nanostructured hydroxyapatite prepared by a spray drying technique. J Res NIST. 2004; 109:543–551.
43. Xu HHK, Moreau JL, Sun L, Chow LC. Nanocomposite containing amorphous calcium phosphate nanoparticles for caries inhibition. Dent Mater. 2011; 27:762–769. [PubMed: 21514655]
44. Moreau JL, Sun L, Chow LC, Xu HHK. Mechanical and acid neutralizing properties and inhibition of bacterial growth of amorphous calcium phosphate dental nanocomposite. J Biomed Mater Res Part B. 2011; 98:80–88.
45. Ruan-antury JD, Gomes JC, Uribe-echevarria J, Gomes OMM. Analysis "in vitro" of the bond strength of self-etch adhesive systems with the dentinal substrate after the dentin deproteinization. Actas Odontológicas. 2006; 3:60–69.
46. Antonucci JM, O'Donnell JN, Schumacher GE, Skrtic D. Amorphous calcium phosphate composites and their effect on composite-adhesive-dentin bonding. J Adhes Sci Technol. 2009; 23:1133–1147. [PubMed: 19696914]
47. McBain AJ. In vitro biofilm models: an overview. Adv Appl Microbiol. 2009; 69:99–132. [PubMed: 19729092]
48. Cheng L, Exterkate RA, Zhou X, Li J, ten Cate JM. Effect of galla chinensis on growth and metabolism of microcosm biofilms. Caries Res. 2011; 45:87–92. [PubMed: 21346356]
49. McBain AJ, Sissons C, Ledder RG, Sreenivasan PK, De Vizio W, Gilbert P. Development and characterization of a simple perfused oral microcosm. J Appl Microbiol. 2005; 98:624–634. [PubMed: 15715865]
50. Antonucci JM, Zeiger DN, Tang K, Lin-Gibson S, Fowler BO, Lin NJ. Synthesis and characterization of dimethacrylates containing quaternary ammonium functionalities for dental applications. Dent Mater. 201110.1016/j.dental.2011.10.004
51. Lima JP, Sampaio de Melo MA, Borges FM, Teixeira AH, Steiner-Oliveira C, Nobre Dos Santos M, et al. Evaluation of the antimicrobial effect of photodynamic antimicrobial therapy in an in situ model of dentine caries. Eur J Oral Sci. 2009; 117:568–574. [PubMed: 19758254]

52. Tyas MJ, Anusavice KJ, Frencken JE, Mount GJ. Minimal intervention dentistry - a review FDI commission project 1–97. Int Dent J. 2000; 50:1–12. [PubMed: 10945174]

53. Frencken JE, van't Hof MA, van Amerongen WE, Holmgren CJ. Effectiveness of single-surface ART restorations in the permanent dentition: a meta-analysis. J Dent Res. 2004; 83:120–123. [PubMed: 14742648]

54. Duarte SJ, Lolato AL, de Freitas CR, Dinelli W. SEM analysis of internal adaptation of adhesive restorations after contamination with saliva. J Adhes Dent. 2005; 7:51–56. [PubMed: 15892364]

55. Loguercio AD, Reis A, Bortoli G, Patzlaft R, Kenshima S, Rodrigues Filho LE, et al. Influence of adhesive systems on interfacial dentin gap formation in vitro. Oper Dent. 2006; 31:431–441. [PubMed: 16924983]

56. Prati C, Fava F, Gioia DDi, Selighini M, Pashley DH. Antibacterial effectiveness of dentin bonding systems. Dent Mater. 1993; 9:338–43. [PubMed: 7988764]

57. Slenters TV, Hauser-Gerspach I, Daniels AU, Fromm KM. Silver coordination compounds as light-stable, nano-structured and anti-bacterial coatings for dental implant and restorative materials. J Mater Chem. 2008; 18:5359–5362.

58. Braga RR, Meira JB, Boaro LC, Xavier TA. Adhesion to tooth structure: A critical review of "macro" test methods. Dent Mater. 2010; 26:e38–e49. [PubMed: 20004960]

59. Triolo PT, Swift EJ, Barkmeier WW. Shear bond strengths of composite to dentin using six dental adhesive systems. Oper Dent. 1995; 20:46–50. [PubMed: 8700770]

60. Pecora N, Yaman P, Dennison J, Herrero A. Comparison of shear bond strength relative to two testing devices. J Prosthet Dent. 2002; 88:511–515. [PubMed: 12474001]

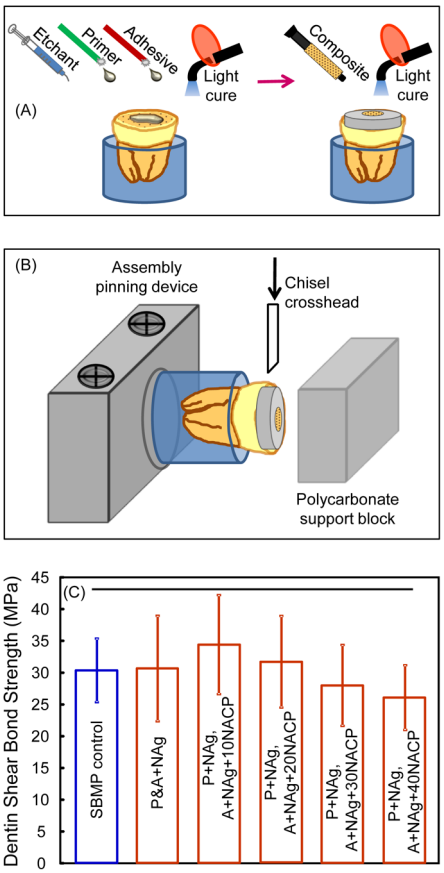

Fig 1.

Dentin shear bond testing. (A) Schematic of specimen preparation, (B) schematic of testing, (C) human dentin shear bond strengths. Each value is mean ± sd (n = 10). Horizontal line indicates values that are not significantly different from each other ($p > 0.1$).

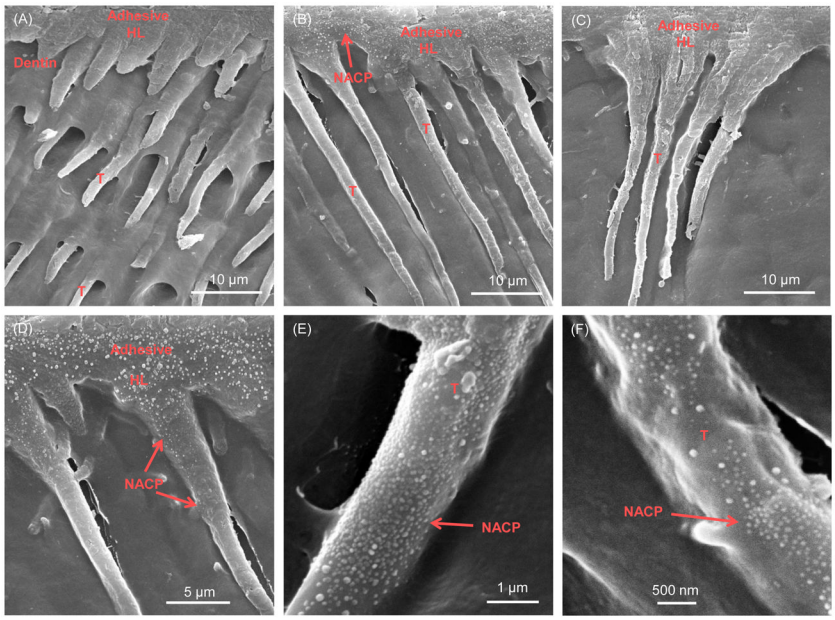

Fig 2.

Representative SEM micrographs of dentin-adhesive interfaces. (A) SBMP control, (B) P +NAg, A+NAg+20NACP, (C) P+NAg, A+NAg+40NACP. (D) P+NAg, A+NAg+20NACP at a higher magnification, and (E, F) at even higher magnifications. Adhesives filled the dentinal tubules and formed resin tags “T” for all six groups. “HL” indicates the hybrid layer between the adhesive and the underlying mineralized dentin. High magnification SEM in (D–F) revealed numerous NACP nanoparticles in the adhesive layer, in the hybrid zone, and inside the dentinal tubules. Arrows in (D–F) indicate NACP in the dentinal tubules. NACP were not only able to infiltrate with the adhesive into straight tubules (E), but also into bent and irregularly-shaped tubules (F).

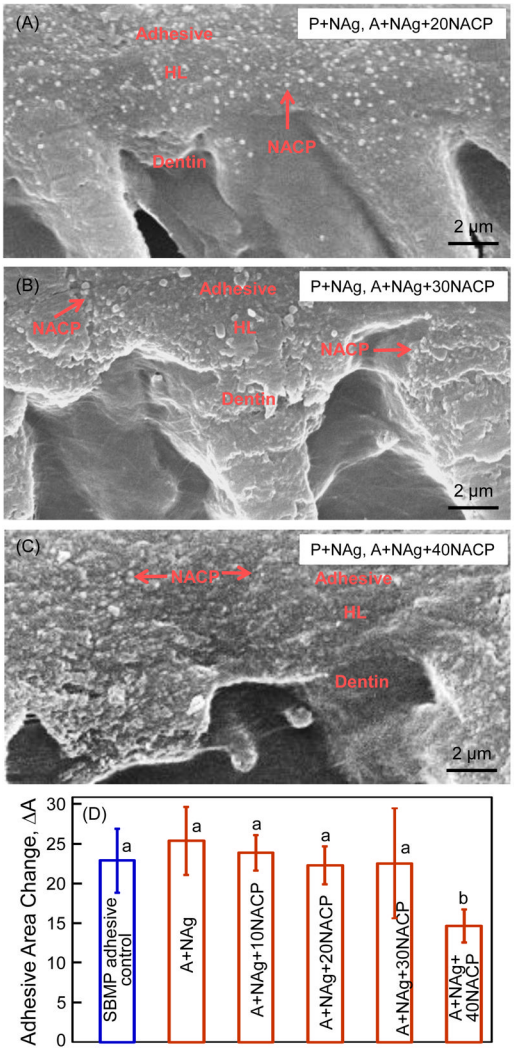

Fig 3.

Representative SEM images of adhesive/hybrid layers at a higher magnification: (A) 20%, (B) 30% and (C) 40% of NACP. NACP in the adhesive and hybrid layers were more readily visible at 20% NACP than at 30% and 40% NACP. However, the NACP were present in the adhesive and hybrid layers at 30% and 40% NACP, as indicated by the arrows. (D) The flow of the adhesive pastes (mean ± sd; n = 6). Flow is inversely related to the viscosity, with a larger adhesive area after flow indicating a lower viscosity. Values with dissimilar letters are significantly different from each other ($p < 0.05$).

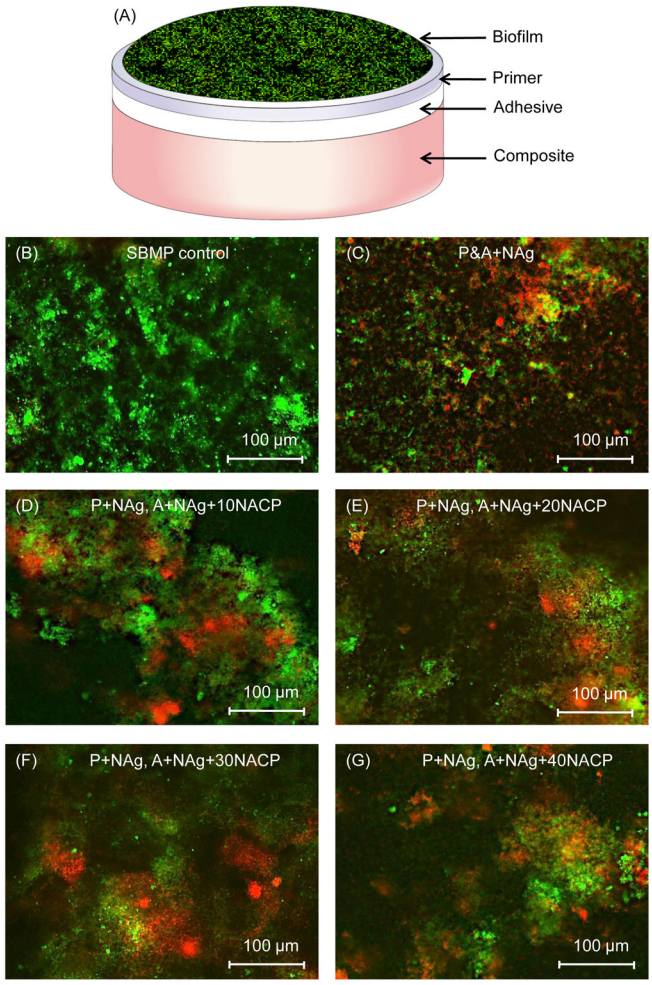

Fig 4.

Dental plaque microcosm biofilm testing and live/dead assay. (A) Schematic of biofilm on the layered specimen, (B–G) live/dead images for the six groups. Live bacteria were stained green, and dead bacteria were stained red. Live and dead bacteria in the proximity of each other produced yellow/orange colors. SBMP control disks were covered with live biofilms. A&P+NAg, with or without NACP, had mostly dead bacteria on the specimens. Therefore, the modified bonding agents with NAg and NACP possessed a potent antibacterial effect.

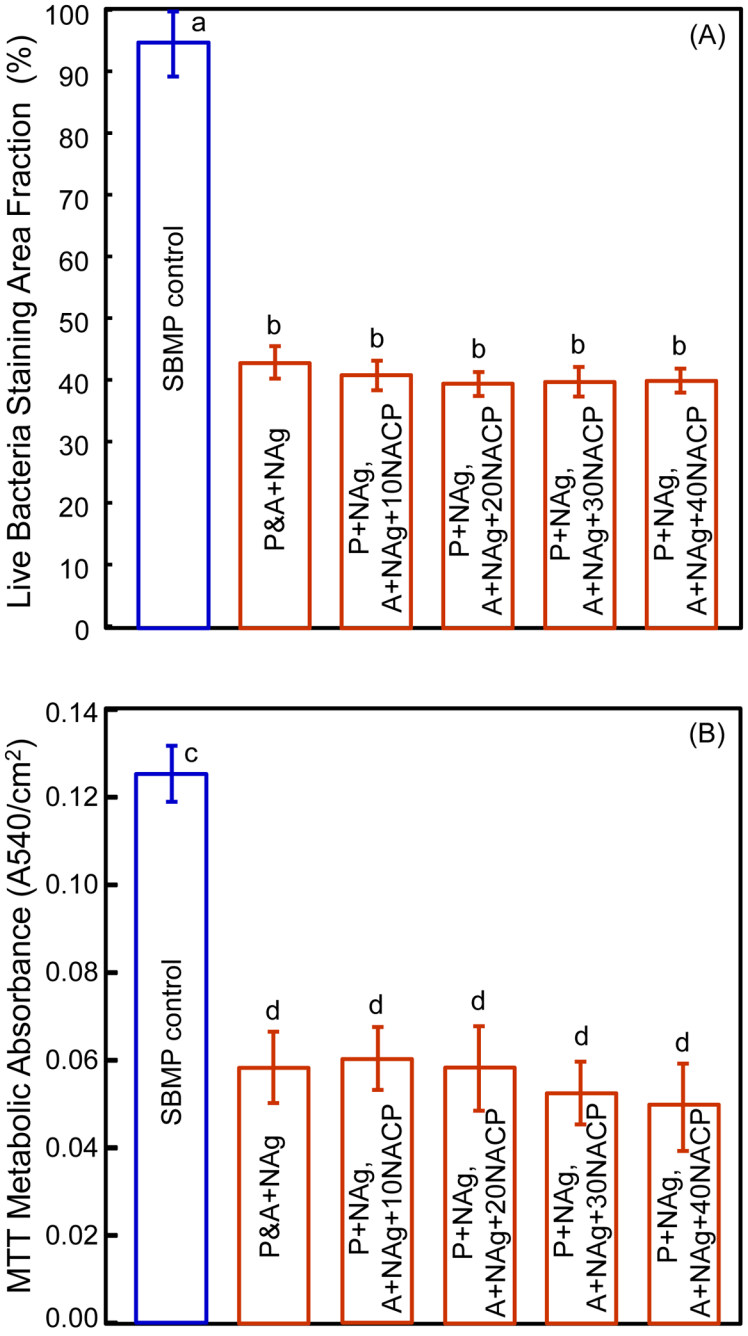

Fig 5.

(A) Live bacteria area fraction, and (B) MTT assay of metabolic activity. Each value is mean ± sd (n = 6). In each plot, the same letters indicates values that are not significantly different ($p > 0.1$).

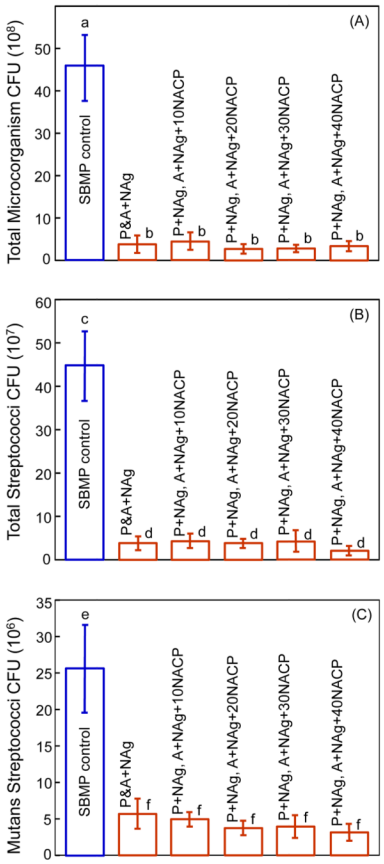

Fig 6.

Biofilm CFU per disk for: (A) Total microorganisms, (B) total streptococci, and (C) mutans streptococci (mean ± sd; n = 6). In each plot, values with dissimilar letters are significantly different ($p < 0.05$).

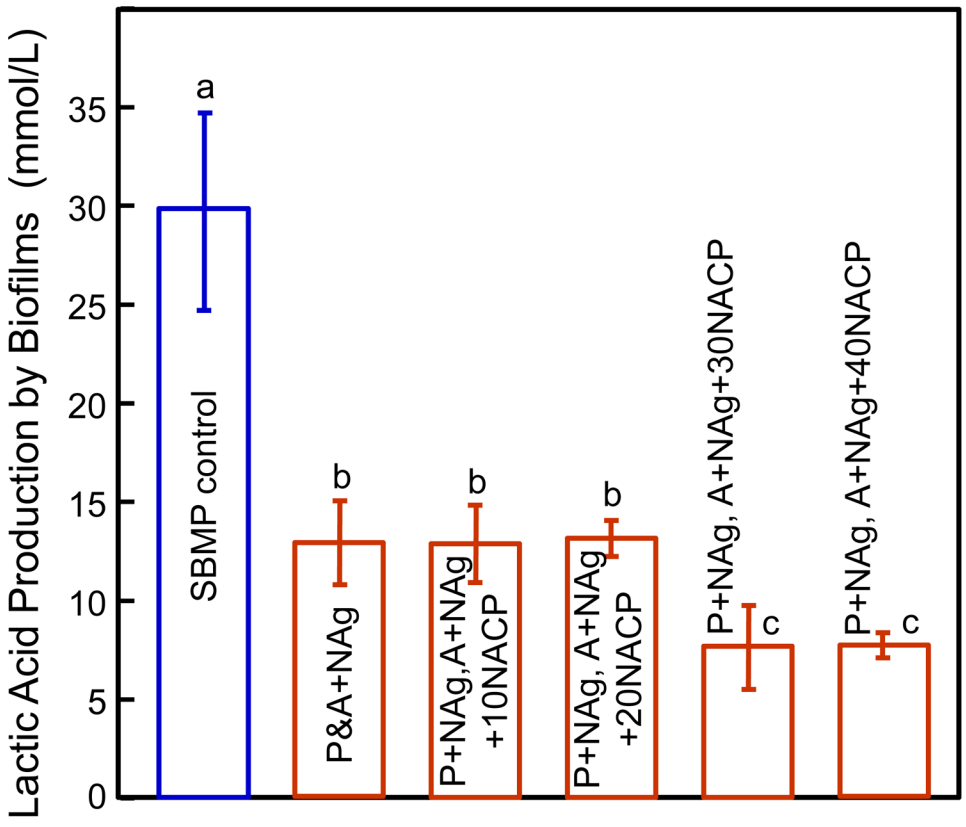

Fig 7.

Lactic acid production by biofilms (mean ± sd; n = 6). Values with dissimilar letters are significantly different ($p < 0.05$). Acid production by biofilms on disks with NAg plus 30% and 40% NACP were approximately 1/4 of that on the control, indicating a potent antibacterial effect.